Physics of the Earth and Planetary Interiors 228 (2014) 203–210

Contents lists available at ScienceDirect

Physics of the Earth and Planetary Interiors

journal homepage: www.elsevier.com/locate/pepi

Elastically accommodated grain-boundary sliding: New insights from experiment and modeling

Ian Jackson [a,*], Ulrich H. Faul [b], Richard Skelton [a]

[a] Research School of Earth Sciences, Australian National University, Canberra, ACT 0200, Australia
[b] Department of Earth, Atmospheric and Planetary Sciences, Massachusetts Institute of Technology, Cambridge, MA, USA

ARTICLE INFO

Article history:
Available online 26 November 2013

Edited by Mark Jellinek

Keywords:
Grain-boundary sliding
Seismic wave attenuation and dispersion
Viscoelastic relaxation
Creep function

ABSTRACT

Substantial progress is reported towards a reconciliation of experimental observations of high-temperature viscoelastic behaviour of fine-grained materials with the micromechanical theory of grain-boundary sliding. The classic Raj–Ashby theory of grain boundary sliding has recently been revisited – confirming the presence of the following features: (i) at a characteristic period τ_e much less than the Maxwell relaxation time τ_d, a dissipation peak of amplitude $\sim 10^{-2}$ and associated shear modulus relaxation resulting from elastically accommodated sliding on grain boundaries of relatively low viscosity; (ii) at intermediate periods, a broad regime of diffusionally-assisted grain-boundary sliding within which the dissipation varies with period as $Q^{-1} \sim T_o^{\alpha}$ with $\alpha \sim 1/3$, sliding being limited by stress concentrations at grain corners, that are progressively eroded with increasing period and diffusion distance; and (iii) for periods longer than the Maxwell relaxation time τ_d, diffusionally accommodated grain-boundary sliding with $Q^{-1} \sim T_o$. For periods $T_o \gg \tau_e$, laboratory dissipation data may be adequately described as a function of a single master variable, namely the normalised period T_o/τ_d. However, it is becoming increasingly clear that the lower levels of dissipation measured at shorter periods deviate from such a master curve – consistent with the existence of the two characteristic timescales, τ_e and τ_d, for grain-boundary sliding, with distinct grain-size sensitivities. New forced-oscillation data at moderate temperatures (short normalised periods) provide tentative evidence of the dissipation peak of elastically accommodated sliding. Complementary torsional microcreep data indicate that, at seismic periods of 1–1000 s, much of the non-elastic strain is recoverable – consistent with substantial contributions from elastically accommodated and diffusionally assisted grain-boundary sliding.

1. Theory of elastically accommodated grain-boundary sliding

In the classic theory of grain-boundary sliding (Raj and Ashby, 1971), the low effective viscosity of grain-boundary regions plays a vital role, as follows. At sufficiently low temperatures and short timescales of stress application, the behaviour of a stressed bi-crystal is strictly elastic (Fig. 1a). However, with increasing temperature and/or timescale of stress application, the low effective viscosity of the boundary region allows a finite amount of slip between adjacent grains. Slip on the periodic corrugated interface between the grains results in a spatially variable normal stress acting across the boundary. This normal stress is responsible for an elastic distortion of the grains that facilitates sliding by eliminating the incompatibilities in grain shape and provides the restoring force for recovery of the non-elastic strain on removal of the applied stress, so that the resulting behaviour is anelastic (Fig. 1b). The characteristic timescale τ_e for such anelastic relaxation by elastically accommodated grain-boundary sliding is given by the expression (e.g., Kê, 1947; Nowick and Berry, 1972):

$$\tau_e = \eta_{gb} d/G_U \delta = \eta_{gb}/G_U \alpha_b \quad (1)$$

The thin grain-boundary region, of thickness δ and length in the sliding direction comparable with the grain size d (and hence of aspect ratio $\alpha_b = \delta/d$), is characterised by atomic positional disorder and, commonly, chemical complexity relative to the adjacent crystalline grains (e.g., Drury and Fitz Gerald, 1996; Hiraga et al., 2003; Faul et al., 2004). This grain-boundary region is assumed to respond to applied stress as a Newtonian fluid, in which the shear stress is the product of strain-rate and a viscosity $\eta_{gb} \ll \eta_{ss}$, the viscosity associated with steady-state diffusional creep of the polycrystal. The two viscosities are expected to have distinctive Arrhenian temperature dependencies. In Eq. (1), G_U is the unrelaxed shear modulus. Under conditions of sinusoidally time-varying shear stress, a dissipation peak and associated partial relaxation of the shear modulus are expected for an angular frequency $\omega \sim 1/\tau_e$.

* Corresponding author.
E-mail address: Ian.Jackson@anu.edu.au (I. Jackson).

0031-9201/$ - see front matter © 2013 Elsevier B.V. All rights reserved.
http://dx.doi.org/10.1016/j.pepi.2013.11.014

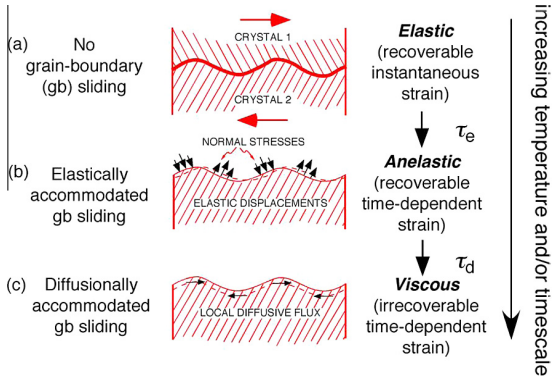

Fig. 1. The concepts that underpin the classic Raj–Ashby model of grain-boundary sliding (redrawn after Ashby, 1972). Regimes (b) and (c) are the domains of elastically accommodated and diffusionally accomodated grain-boundary sliding, respectively. Intervening between these two regimes is that of diffusionally assisted grain-boundary sliding. Within this latter regime, the distribution of boundary-normal stress is progressively modified by diffusion from that pertaining on completion of elastically accommodated sliding, involving stress concentrations at grain corners, to the parabolic distribution appropriate for steady-state creep (Raj, 1975).

At higher temperatures and/or longer timescales of stress application, the distribution of boundary-normal stress is modified by diffusional transport of matter along the grain boundary, ultimately allowing the transition from anelastic towards viscous behaviour (Fig. 1c). The time constant τ_d for the evolution of the distribution of normal stress from that prevailing on completion of elastically accommodated sliding to that associated with steady-state diffusional creep, and thus the duration of transient diffusional creep, was identified (Raj, 1975), within a dimensionless multiplicative factor, to be the Maxwell time for diffusional creep with the steady-state viscosity η_{ss}, i.e.

$$\tau_d = (1-\nu)kTd^3/(40\pi^3 G_U \delta D_{gb}\Omega) = \eta_{ss}/G_U \quad (2)$$

where ν, k, T, D_{gb}, and Ω are respectively Poisson's ratio, the Boltzmann constant, the absolute temperature, the grain-boundary diffusivity and the molecular volume of the diffusing species. Such transient creep behaviour is adequately described, at least for time intervals of finite duration, by an Andrade creep function (Gribb and Cooper, 1998; Jackson et al., 2006). For sinusoidally time-varying shear stress, such anelastic behaviour results in a weakly frequency/period dependent dissipation and associated modulus relaxation, of the type often referred to as 'high-temperature background' (e.g., Nowick and Berry, 1972).

The classical Raj–Ashby model of grain-boundary sliding has recently been revisited by Morris and Jackson (2009a). The boundary value problem describing sliding on a fixed periodic piecewise linear interface between two elastic grains, including both low effective viscosity of the grain-boundary region and grain-boundary diffusion, was solved in the limit of infinitesimal boundary slope for the complete mechanical relaxation spectrum. A dissipation peak located at $\omega \sim 1/\tau_e$, and the diffusionally accommodated sliding regime with $Q^{-1} \sim \omega^{-1}$ for $\omega < 1/\tau_d$, are separated by a diffusionally-assisted sliding regime within which Q^{-1} varies very mildly (approximately as $1/\log\omega$) with frequency (Fig. 2a). The term 'diffusionally assisted' is used to convey the idea that within this regime, diffusion occurs on progressively greater spatial scales (ultimately comparable with the grain size d) with decreasing frequency towards $1/\tau_d$. The width (in frequency or timescale of stress application) of this diffusionally assisted regime, is determined by ratio $M = \tau_e/\tau_d$, which is poorly constrained a priori, but inferred from experimental data for fine-grained polycrystals to be $\ll 1$ (Morris and Jackson, 2009a).

More recently, a combination of analytical and numerical (finite-element) methods has been used to extend the work of Morris and Jackson (2009a) to finite slopes of the same piecewise linear boundary between elastic grains (Lee and Morris, 2010;

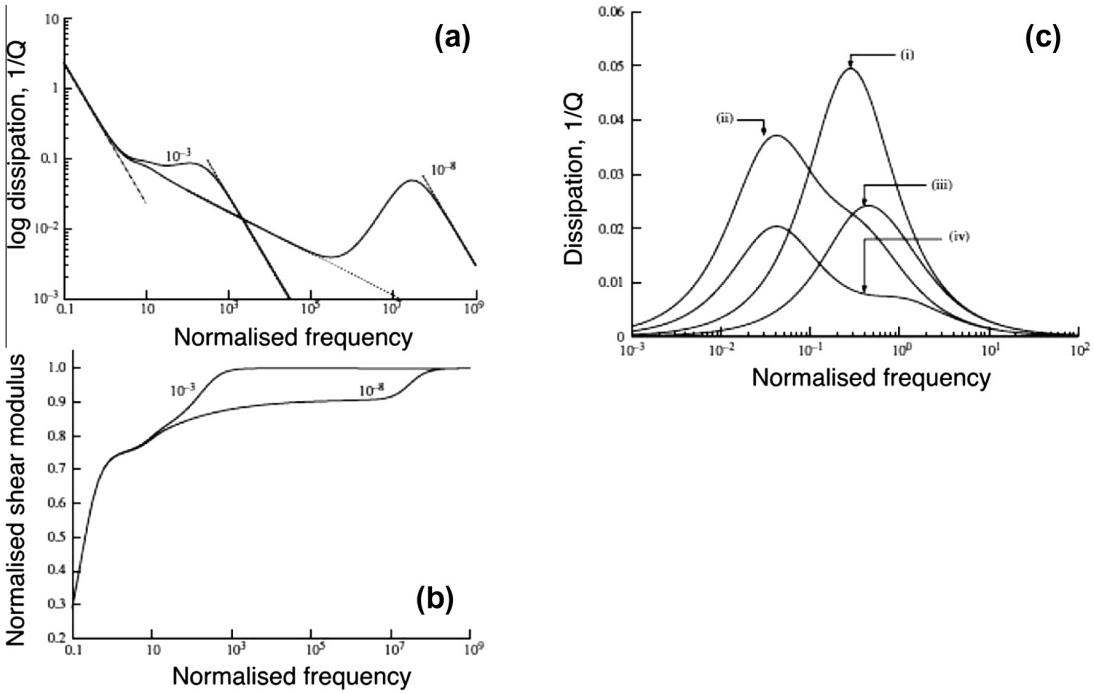

Fig. 2. (a) and (b) The mechanical relaxation spectrum of Lee et al. (2011) for the $\varphi = 30°$ saw-tooth interface, with alternative values of $M = \tau_e/\tau_d$ of 10^{-8} and 10^{-3}. (c) The effect on Q^{-1} of spatial heterogeneity in grain size and/or viscosity (Lee and Morris, 2010, Fig. 9). Curves labelled (i–iv) correspond respectively to uniform grain size and viscosity, 10-fold variation of grain-boundary viscosity, 4-fold variation of grain size, both 10-fold variation of boundary viscosity and 4-fold variation of grain size.

Lee et al., 2011). Anelastic relaxation associated with elastically accommodated sliding was confirmed but with a dissipation peak amplitude ~0.05 more than an order of magnitude lower than that for the infinitesimal-slope solution (Lee and Morris, 2010). Furthermore, it was demonstrated that the peak amplitude decreases only mildly with increase of N, the number of terms retained in the Fourier series approximation to the topography on the piecewise linear periodic boundary. N is a proxy for the sharpness of the grain corners, that had previously invoked as a possible inhibitor of elastically accommodated sliding (Jackson et al., 2006). Increase of N from 10 to ∞ resulted in a decrease of only 30% in the peak dissipation. For a 'saw-tooth' boundary with slope $\varphi = 30°$ within an array of regular hexagons, designed to model local 4-fold variation of grain size, a further 50% reduction in peak amplitude was found (Lee and Morris, 2010; Fig. 2c). A local 10-fold variation in viscosity along a similar boundary resulted in a 25% reduction of peak dissipation along with broadening by an order of magnitude in frequency. In combination, these variations resulted in a height of 0.02 for the broadened peak associated with elastically accommodated sliding (Lee and Morris, 2010; Fig. 2c).

For the diffusionally-assisted grain-boundary sliding regime with finite boundary slopes, the dissipation was found to exhibit a power-law dependence on normalised frequency i.e. $Q^{-1} = A(\omega\tau_d)^{-\alpha}$. The power law exponent α depends only upon the slope φ of the boundary through the relationship $\alpha = (2/3)(1 - \lambda(\varphi))$, where λ with values between 0 and 1 is a measure of the stress concentration at the grain corner. For the saw-tooth boundary with $\varphi = 30°$, $\alpha = 0.3$. The proportionality constant A depends upon the orientation of the boundary relative to the stress field. The dissipation decreases markedly with increasing boundary slope, by about a factor of 10 for an increase from 0.36° to 30° (Lee et al., 2011). For a piecewise linear boundary involving corners subtending different angles, the behaviour is more complicated, but at high frequencies, the dissipation is well approximated by a power-law with an exponent corresponding the largest subtended angles (Lee et al., 2011, Fig. 8).

In summary, the qualitative features predicted by the infinitesimal-slope analysis of Morris and Jackson (2009a) survive when the interface has finite slope, but the overall level of dissipation is greatly reduced and depends strongly on slope (Fig. 2). The dissipation is still controlled by stress concentrations near corners on the interface, with the energy dissipation at each corner dependent upon the angle subtended by the corner, and on the local orientation of the interface relative to the principal axes of applied stress.

Such micromechanical models of grain-boundary sliding thus clearly predict that the first significant indication, with increasing temperature, of the breakdown of strictly elastic behaviour in fine-grained materials should be a broad dissipation peak with amplitude of order 10^{-2} and associated modulus dispersion, reflecting anelastic behaviour associated with elastically accommodated grain-boundary sliding. With further increase in period and/or temperature, diffusion will become progressively more influential, allowing first, additional anelastic strain within the diffusionally assisted sliding regime, and ultimately the irrecoverable viscous strain of diffusionally accommodated grain-boundary sliding.

2. Master-variable scaling of viscoelastic relaxation?

Most recent laboratory work, for example on polycrystalline olivine, has been performed on polycrystals of grain size no more than a few tens of μm. Only such fine-grained materials can be cycled through wide ranges of temperature without microcracking by intergranular stresses resulting from anisotropic thermal expansivity of the constituent crystallites. However, for seismological application, such data concerning low-strain viscoelastic behaviour need to be extrapolated to the mm–cm grainsizes expected of mantle rocks. In the previous section, the viscoelastic behaviour associated with grain boundary sliding was shown to have two characteristic timescales τ_e and τ_d, each with its own distinct grain-size sensitivity. However, it has been argued that at least for restricted ranges of period, temperature and grain size, the viscoelastic behaviour can in fact be described by a single normalised period/frequency (Gribb and Cooper, 1998; Morris and Jackson, 2009b). Morris and Jackson (2009b) emphasised that demonstration of such similitude would prove that the viscoelastic behaviour can be understood entirely in terms of grain-scale diffusion. This idea of scaling of frequency (or equivalently, period) with the Maxwell relaxation time τ_d calculated though Eq. (2) from the viscosity measured in an independent microcreep test has been reinforced by the recent study of McCarthy et al. (2011). These authors showed that selected forced-oscillation data (restricted to relatively high levels of dissipation: $\log Q^{-1} > -1.4$) for various materials are adequately described by a master curve specifying Q^{-1} as a unique function of normalised frequency.

In contrast, Jackson and Faul (2010) have advocated an approach to the fitting of experimental forced-oscillation data with an extended Burgers model, in which the relaxation times associated with anelastic and viscous behaviour are allowed distinct grain-size sensitivities. Incorporation of a broad low-amplitude dissipation peak and associated modulus dispersion – plausibly attributed to elastically accommodated grain-boundary sliding – provides a seamless transition between (unrelaxed) elastic behaviour and the low-frequency forced-oscillation data. The dataset for essentially dry, melt-free olivine that was fitted by Jackson and Faul (2010) yielded a mild grain-size sensitivity for the anelastic relaxation times ($\tau_e \sim d^{1.3}$) but no constraint on the grain-size sensitivity for τ_d. Accordingly, we set $\tau_d = \eta/G_U \sim d^3$ – consistent with Coble creep involving grain-boundary diffusion. These data, augmented by the results of recent work on a newly prepared San-Carlos-derived olivine polycrystal of 16.6 μm average grain size, reach dissipation values as low as $\log Q^{-1} = -2.5$, and thus approach much more closely the threshold for genuinely elastic behaviour, than does the dataset of McCarthy et al. (2011) limited to $\log Q^{-1} > -1.4$. It is evident from Fig. 3b that these data reveal much milder grain-size sensitivity of dissipation than is prescribed by scaling the oscillation period with the Maxwell time τ_d with the expected d^3 dependence upon grain size. Only if the grain-size exponent for viscosity used to calculate the normalised period is arbitrarily reduced to 1.3, the value well-constrained within the extended Burgers model for the anelastic relaxation times, do the data collapse more nearly onto a single curve. The implication is that a grain-size exponent of viscosity markedly lower than the range of 2–3 expected for diffusional creep would need to be invoked to approach a satisfactory single-master-variable scaling of oscillation period.

Until recently, it had been our assumption that the dislocation densities in our hot-pressed specimens are sufficiently low as to contribute negligibly to the viscoelastic relaxation. However, it has recently been demonstrated (Farla et al., 2012) that dissipation increases systematically with increasing dislocation density for a suite of fine-grained, hot-pressed and pre-deformed olivine polycrystals. It follows that the dislocation densities for hot-pressed, but otherwise undeformed, material are apparently sufficient to make an appreciable contribution to the observed viscoelastic relaxation. Such grain-size-insensitive dislocation-related relaxation, operating in parallel with grain-boundary relaxation, would tend to result in milder grain-size sensitivity, than for the grain-boundary processes acting alone.

Forced-oscillation data for synthetic peridotite (olivine-orthopyroxene mixtures) have similarly been attributed to grain-boundary

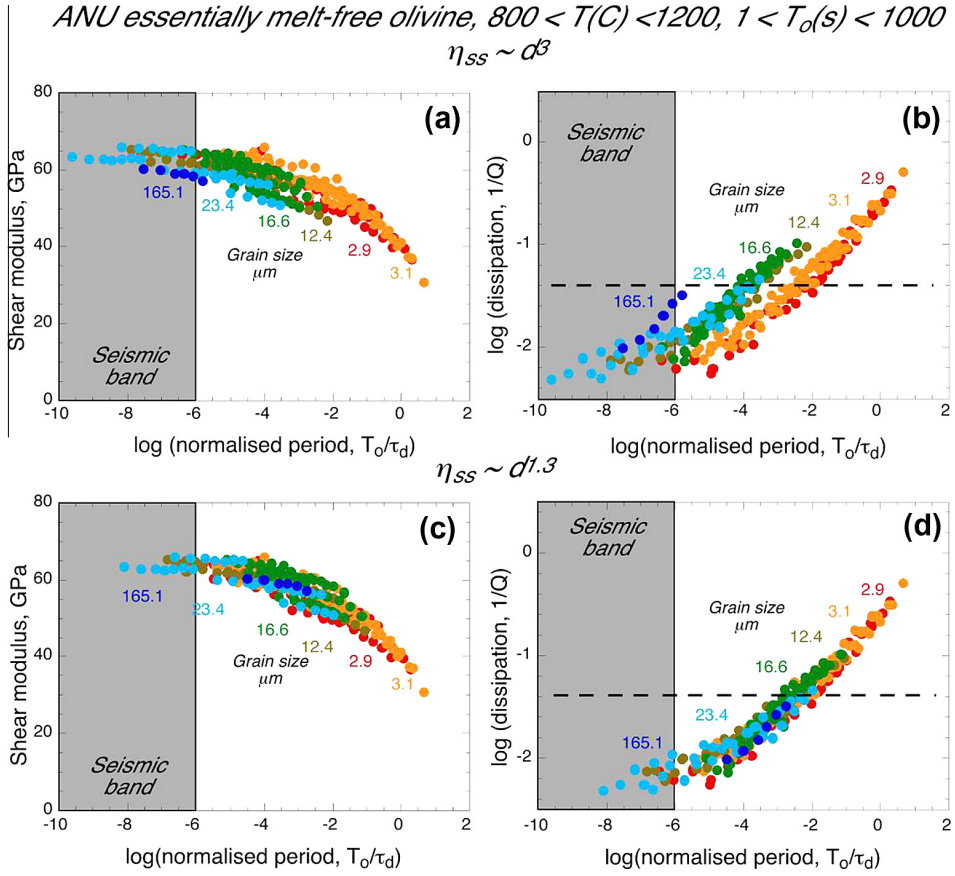

Fig. 3. Re-assessment of master-variable scaling of shear modulus and dissipation for ANU data for specimens of essentially dry, melt-free polycrystalline olivine tested at temperatures of 800–1200 °C and oscillation periods of 1–1000 s. The four-specimen dataset analysed by Morris and Jackson (2009b) has been revised and expanded to incorporate data for temperatures in the range 800–950 °C (Jackson and Faul, 2010); moreover, data for two additional olivine specimens of 3.1 μm grain size (Jackson and Faul, 2010) and 16.6 μm grainsize, have been included. In panels (a) and (b), the oscillation period is scaled with the relaxation time τ_d which varies with grain size d and temperature T as $\tau_d = \eta_{ss}(d,T)/G_U \sim d^3\exp(E/RT)$ as expected for Coble creep. Panels (c) and (d) demonstrate a closer approach to collapse of the data onto a master curve if the timescale τ_d used for scaling varies with grain size as $d^{1.3}$. The dashed lines in panels (b) and (d) represent the lower limit $(\log Q^{-1}) = -1.4$ of the data used by McCarthy et al. (2011) to assess the validity of a model in which dissipation is a function only of frequency (or period) normalised by the Maxwell time.

sliding with a mixture of elastic and diffusional accommodation (Sundberg and Cooper, 2010). These authors chose to model the high-temperature background dissipation for a synthetic peridotite with an Andrade creep function, with a superimposed dissipation peak attributed to elastically accommodated sliding and modelled with a single anelastic relaxation time. A similar conclusion concerning the breakdown of master-variable scaling of period/frequency with the Maxwell time has recently been reported by Takei and Karasawa (2012) for the organic silicate analogue material borneol newly tested at lower levels of dissipation.

It is therefore concluded that scaling with the Maxwell time is effective only for conditions far removed from the elastic/anelastic threshold where normalised periods approach or exceed unity. The neglect of the systematically milder grain-size sensitivity of Q^{-1} under low-loss conditions at short normalised periods (or high normalised frequencies), that is implicit in this approach, will result in misleading extrapolations to the conditions of seismic wave propagation in the Earth's upper mantle.

The foregoing discussion serves to highlight the need for further laboratory experiments that more closely scrutinise the onset of the high-temperature transition from elastic behaviour in fine-grained materials. In the following sections, we present new experimental observations for fine-grained polycrystalline olivine that (i) strengthen the circumstantial evidence for a broad, low-amplitude dissipation peak at moderate temperatures, diagnostic of elastically accommodated grain-boundary sliding, and (ii) constrain the fraction of recoverable non-elastic strain – attributable to elastically accommodated and diffusionally-assisted grain-boundary sliding.

3. Insights from preliminary forced-oscillation observations on copper-jacketted olivine

In the experimental assembly normally used for forced-oscillation experiments under conditions of simultaneously high pressure (200 MPa) and temperature (to 1300 °C) in our ANU laboratory, an olivine specimen of 30 mm length and 11.5 mm diameter wrapped in $Ni_{70}Fe_{30}$ foil, is sandwiched between torsion rods of high-grade polycrystalline alumina within a thin-walled jacket of mild steel. The jacket, sealed with an *O*-ring at each end, beyond the furnace hot-zone, serves to isolate the specimen from the argon pressure medium, thereby ensuring frictional coupling between the specimen and torsion rods. The high melting point and low thermal conductivity of mild-steel jacket material allow routine access to temperatures in excess of 1200 °C. However, the occurrence of the sluggish phase transition between the austenite (face-centred cubic) and ferrite (body-centred cubic) phases during cooling from ~900 to <700 °C results in strongly viscoelastic behaviour of the jacket material though this temperature interval, that varies with

thermal history. Such variations in mechanical behaviour of the jacket material complicate the robust determination of the shear modulus G and dissipation $1/Q$ for the enclosed olivine specimen, and thus potentially impede the observation of its transition with decreasing temperature from anelastic to elastic behaviour.

Accordingly, we have trialled the use of copper as an alternative jacket material in some exploratory experiments to 900 °C. For this purpose, the residue of a sol–gel olivine specimen #6585, previously tested in an $Ni_{70}Fe_{30}$ foil-lined steel jacket (Jackson and Faul, 2010) and subsequently sectioned for microstructural characterisation, was precision ground to a length of ~18 mm (c.f. the standard 30 mm), dried by firing at 1200 °C under controlled atmosphere, and loaded without any foil wrapper into a thin-walled copper jacket. The specimen recovered following testing in copper to 200 MPa and 900 °C, was ~4% more porous than its precursor 6585 and less uniform in grain size – some grains having grown to ~20 μm. These microstructural changes are attributed to the long multi-stage history of this specimen including multiple controlled-atmosphere firings at 1400 °C and (most recently) 1200 °C and atmospheric pressure and subsequent annealing under conditions of 200 MPa and either 1200 °C or (most recently) 900 °C.

Following such annealing for a total of 50 h in two successive excursions to 900 °C, torsional forced-oscillation and microcreep tests were performed during slow staged cooling to room temperature. Similar torsional oscillation experiments were performed on a reference assembly in which a sapphire crystal replaced the olivine specimen. Subtraction of the complex torsional compliance of the reference assembly from that of the olivine specimen assembly allowed elimination of the unwanted contribution of the torsion rods.

For a sapphire control specimen oriented with [0 0 1] parallel with the torsional axis, the relevant elastic shear modulus for torsional loading is $G = c_{44} - 2c_{14}^2/(c_{11} - c_{12})$ (Voigt, 1883, cited by Liebisch, 1891). Temperature-dependent values of G were calculated from published ultrasonic (high-frequency) data for the temperature dependence of the single-crystal elastic constants c_{ij} (Anderson and Isaak, 1995). The viscoelastic behaviour of the copper was investigated in companion experiments in which a copper specimen was encapsulated in a copper jacket. The shear modulus and dissipation for the copper specimen were determined with trial values of these quantities for the copper jacket – with iteration to consistency between the properties of the jacket and specimen (as previously described for steel, Jackson et al., 2000).

The parallel processing of torsional forced-oscillation data for the Cu-jacketted olivine specimen assembly and the Cu-jacketted sapphire reference asembly, thus yields generally systematic variations of shear modulus and dissipation for the olivine specimen (Fig. 4). With a maximum temperature of 900 °C (conservatively below the melting temperature of 1084 °C for pure copper), the measured dispersion of the shear modulus and associated dissipation are both limited. The temperature dependence of G is somewhat scattered for temperatures between 900 and 600 °C – reflecting the impact of uncertainties in the calibration factors for the torsional mode displacements for both specimen and reference assemblies. The dissipation data are also somewhat scattered as expected at such low levels of dissipation ($Q^{-1} \leqslant 0.02$) – but relatively coherent trends are observed at the highest temperatures (800–900 °C). These $\log Q^{-1}$ vs $\log T_o$ trends have a generally consistent shape – suggestive of the superposition of a broad dissipation peak upon a monotonically positive background (Fig. 4). In order to further explore this possibility, the 20 (G,Q^{-1}) pairs for the temperature range 800–900 °C having $\log Q^{-1} \geqslant -2.8$ have been tentatively fitted to extended Burgers models (Jackson and Faul, 2010) with and without a dissipation peak and associated modulus relaxation. Such a dissipation peak and the associated dispersion, is modelled as in Jackson and Faul (2010), by augmenting the distribution of anelastic relaxation times specified by Eq. (9) of that publication with the separately normalised distribution:

$$D_p(\ln \tau) = \sigma^{-1}(2\pi)^{-1/2} \exp\{-[\ln(\tau/\tau_p)/\sigma]^2/2\} \quad (3)$$

with relaxation strength δ_P. The 'peak' anelastic relaxation time τ_P is related to the corresponding quantity τ_{PR} at the reference temperature T_R by the Arrhenian expression

$$\tau_p(T) = \tau_{PR} \exp\{(E_P + PV_P)(1/T - 1/T_R)/R\} \quad (4)$$

in which E_P and V_P are respectively the activation energy and activation volume, P the pressure and R the gas constant. Incorporation of such a dissipation peak results in a substantially improved fit to these somewhat scattered data with the following refined values for the model parameters: $\delta_P = 0.016$ (2), $\log \tau_{PR} = 1.15$ (7), and $E_P = 259$ (25) kJ mol^{-1}, with T_R fixed at 900 °C, V_P at 10 cm^3 mol^{-1}, and the peak width parameter σ at 0.9. The results of these exploratory experiments with a copper jacket are broadly consistent with those previously reported for the same specimen tested within a steel jacket – especially with allowance for the previously mentioned microstructural changes. The new data provide further tantalising, but not yet definitive, evidence of a dissipation peak attributable to elastically accommodated grain-boundary sliding, superimposed on a generally steeper monotonic background.

The inferred value for the timescale τ_P for the dissipation peak, although preliminary, can be used in Eq. (1) to estimate the

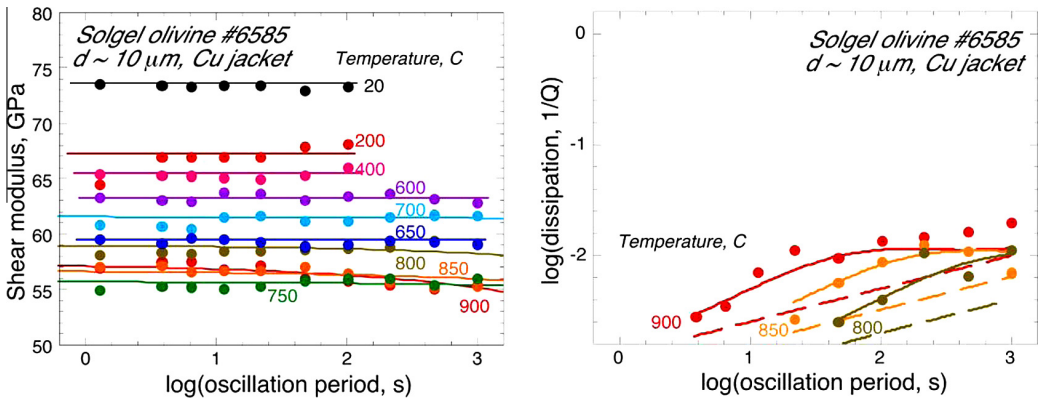

Fig. 4. Shear modulus and dissipation from torsional forced-oscillation measurements on copper-jacketted olivine #6585. The broken and solid curves in the right-hand panel represent the background-only and background + peak dissipation as modelled by the optimal extended Burgers model fit (see text for details).

grain-boundary viscosity η_{gb}. For a plausible boundary aspect ratio α_b of 10^{-4}, corresponding to a grain boundary width δ of 1 nm with a grainsize of 10 μm, η_{gb} is inferred to be $\sim 10^8$ Pa s at 900 °C. The activation enthalpy $H_P = E_P + PV_P$, constrained by data obtained in this study at 800–900°, provides the basis for a speculative extrapolation to higher temperatures. The result is a grain-boundary viscosity for pure Fo_{90} olivine of order 10^5 Pa s at 1200–1300 °C that is, not unreasonably, substantially higher than those (1–100 Pa s) for basaltic melt at similar temperatures (Murase and McBirney, 1973).

Dissipation peaks, of similar amplitude 0.01–0.04 varying inversely with grain size and superimposed upon a monotonic background, have been observed at high temperatures in resonance studies (at 1–30 Hz) of comparably pure, fine-grained (3–23 μm) MgO and Al_2O_3 polycrystals (Pezzotti, 1999). Grain boundary viscosities of $10^{6.5}$–10^9 Pa s for temperatures of 1300–1800 °C were inferred for these materials from the frequencies ($1/\tau_P$) at which the dissipation peaks were observed.

Follow-up experiments are planned in which we will seek to reach higher temperatures (possibly 1050 °C) in copper jackets with newly prepared olivine specimens of optimal microstructure. Such data should allow more definitive resolution of the proposed dissipation peak and closer comparison with the previous measurements in steel jackets.

4. Microcreep tests and the recoverability of viscoelastic strain

Torsional forced-oscillation tests involving an integral number of complete oscillation periods provide no opportunity to assess the extent to which any non-elastic strain is anelastic, i.e. recovered following removal of the applied torque. However, such information is available through complementary torsional microcreep tests of total duration typically either 5000 or 10,000 s, comprising five segments of equal duration during which the torque successively assumes the constant values 0, +L, 0, −L, 0, respectively (Jackson, 2000; see also Gribb and Cooper, 1998). The first segment is used to estimate and correct for any linear drift, leaving a 4-segment record of duration T within which the torque is switched at times usually $t_i = (i-1)T/4$, $i = 1,4$. The successive switchings of the torque can be modelled as the superposition of Heaviside step functions of appropriate sign s_i (+1 @ t_1 and t_4, −1 @ t_2 and t_3).

Provided that the viscoelastic behaviour is linear, the time-dependent twist per unit torque of the experimental assembly $S(t)$ for $0 < t < T$ is appropriately modelled as the superposition of the responses to each of the torque switching events. For reasons of parametric economy, the Andrade creep function $J(t)$ is here preferred over the extended Burgers model to specify the response of the system at time t to the application of the Heaviside step-function torque $H(t)$ at time $t = 0$:

$$J(t) = H(t)[J_U + \beta t^n + t/\eta], \tag{5}$$

where the Heaviside function $H(t)$ is specified as usual as:

$$H(t) = 0, \text{for} -\infty < t < 0, \text{and } H(t) = 1, \text{for } 0 \le t < \infty. \tag{6}$$

The Andrade creep function prescribes infinite strain rate at $t = 0$, and a transient strain that is unbounded as $t \to \infty$ (e.g., Jackson, 2000). The latter is a major disadvantage for extrapolation to very long timescales, and may also bias the analysis of strain recoverability in experimental microcreep records of finite duration. An alternative strategy involving the simultaneous fitting of a creep function of extended Burgers type to both forced-oscillation data and complementary microcreep data will be explored in future work.

With allowance for the previously defined sign s_i of the switching of the torque at time t_i, the contribution to the twist per unit torque at time t from the particular episode of torque switching at time t_i is thus:

$$S_i(t) = s_i J(t - t_i), \tag{7}$$

the argument $t - t_i$ being the time delay since the torque switching at $t = t_i$. For any given t, such contributions need to be summed over all prior switchings of the torque, so that:

$$S(t) = \sum_{(i=1,4)} S_i(t) = \sum_{(i=1,4)} s_i J(t - t_i). \tag{8}$$

Time-domain processing of the microcreep records involves refining the values of the Andrade creep function parameters J_U, β, n and η by non-linear least squares to provide the optimal fit to $S(t)$ the measured twist per unit torque.

As for forced-oscillation data, torsional microcreep records are compared with those from parallel tests on a reference assembly containing an alumina control specimen – thus allowing subtraction of the unwanted contribution from the distortion of the torsion rods. Following recognition of the significant role played by the finite compliance of the interfaces between torsion rods and specimen (Jackson et al., 2009), microcreep data for a reference assembly containing a pair of $Ni_{70}Fe_{30}$ foils at one end of the control specimen have been employed in the present analysis to provide a clearer indication of the extent to which the non-elastic strain is recoverable. Any difference in duration between the microcreep tests conducted on the specimen and reference assemblies is addressed by fitting an Andrade model to the record for the reference assembly and using it to construct a synthetic microcreep record for the reference assembly that is of the same duration as that for the specimen assembly.

Application of this procedure to a representative microcreep record of 5000 s total duration obtained at 1200 °C for a hot-pressed San Carlos olivine specimen HP6728 of 16.6 μm average grain size is shown in Fig. 5. In order to facilitate the comparison of this microcreep record with a record of greater duration (10,000 s) for the reference assembly, the optimal Andrade model fitted to the latter has been used to construct a synthetic microcreep record of 5000 s duration (Fig. 5). This synthetic record (labelled 'reference ass'y' in Fig. 5) is then subtracted from that for the specimen assembly ('specimen ass'y') to yield the relative microcreep record ('difference spec-ref') also displayed in Fig. 5. Thus far, all processing has been done in the time domain. The optimal time-domain Andrade fit to the 'spec-ref' difference record is then calculated and Laplace-transformed to obtain the corresponding complex dynamic compliance at the periods T_o of our forced-oscillation experiments in the range 1–1000 s. A normally very small correction is then made for any differences in geometry between the two assemblies, to obtain the relative dynamic torsional compliance $S_{RL}(T_o)$. Next, the dynamic torsional compliance $S_{JA}(T_o)$ for the jacketted alumina control specimen, in which the control specimen and jacket act in parallel to support the applied torque, is calculated a priori from complementary forced-oscillation data for steel and an Andrade pseudoperiod model (Jackson et al., 2009) fitted to published data for alumina (Lakki et al., 1998). The sum $S_{RL}(T_o) + S_{JA}(T_o)$ is the dynamic torsional compliance $S_{JR}(T_o)$ of the jacketted rock specimen. The reciprocal of S_{JR} is the torsional stiffness of the jacketted rock specimen, which is then corrected for the stiffness of the jacket (inclusive of foil wrapper), and inverted to obtain the dynamic torsional compliance $S_R(T_o)$.

The values of $S_R(T_o)$ thus calculated at the forced-oscillation periods between 1 and 1000 s are then fitted to an Andrade creep function allowing calculation of the associated microcreep record by superposition of the responses to the successive episodes of torque switching. The results for $S_R(t)$, labelled 'specimen only' are also displayed in Fig. 5.

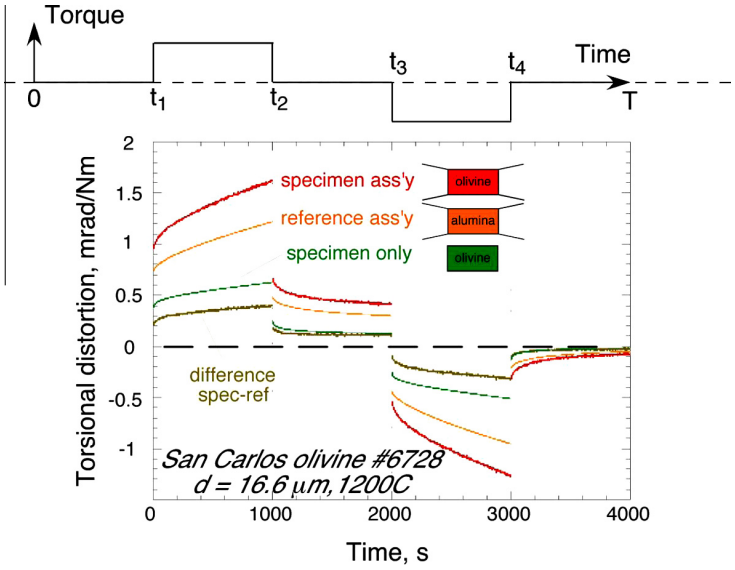

Fig. 5. The time-domain view of the processing of a torsional microcreep record of 5000 s total duration for San Carlos olivine specimen 6728 at 1200 °C.

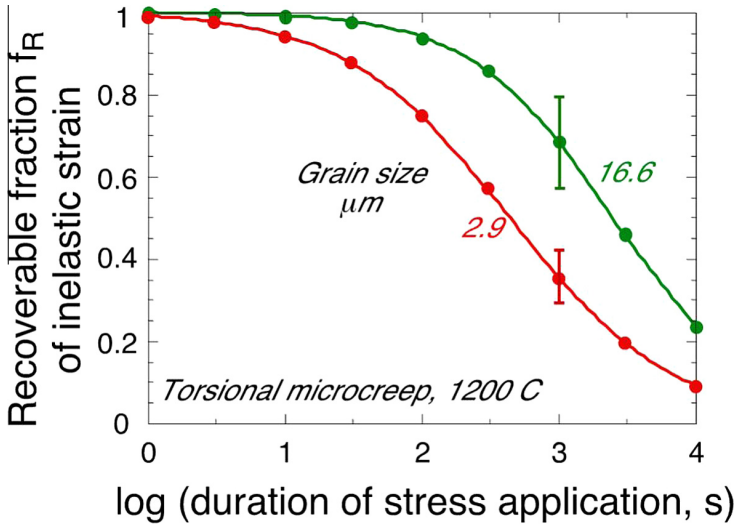

Fig. 6. The recoverable fraction of non-elastic strain estimated from Andrade fits to microcreep data for olivine polycrystals of contrasting grain size. The material-specific quantities n and $\beta\eta$ for the Andrade creep functions fitted to the processed microcreep data $S_R(T_o)$ for the two specimens tested at 1200 °C are as follows: 2.9 µm, 0.26, 90 s^{1-n}; 16.6 µm, 0.15, 774 s^{1-n}. Propagation of the formal uncertainties in the parameters n, β, and η and the covariances among them through to f_R results in the representative error bars attached to the plotting symbols at log (duration) =3.

The recoverable (i.e. anelastic) strain is identified with the βt^n term in the Andrade model, and the fraction f_R of the total inelastic strain $\beta t^n + t/\eta$ can be calculated as a function of the duration t of steady torque application:

$$f_R = \beta t^n/(\beta t^n + t/\eta) = 1/(1 + t^{1-n}/\beta\eta) \quad (9)$$

Such an estimate can be made for the Andrade model fitted to the rather directly determined difference between the microcreep records for the specimen and reference assemblies, or alternatively for the Andrade model fitted to the final $S_R(T_o)$ data. Closely consistent results concerning the recoverable fraction of the non-elastic strain are obtained with these two approaches – though the latter estimate for the specimen itself is preferred.

Such estimates of $f_R(t)$ are displayed in Fig. 6 for polycrystalline olivine specimens of two contrasting grain sizes. It is evident that for torque application on the timescales of teleseismic periods, much of the inelastic strain will be recoverable – consistent with contributions from both elastically accommodated and diffusionally assisted grain-boundary sliding, and that the recoverable fraction f_R increases with increasing grain size.

5. Conclusions and prospects

The long-sought reconciliation of the theory of grain-boundary sliding with experimental observations is within reach. Recent micromechanical modelling of grain-boundary sliding confirms the prediction of a dissipation peak at $T_o \sim \tau_e$ associated with recoverable, elastically accommodated sliding on grain boundaries of low effective viscosity (Morris and Jackson, 2009a). However, the subsequent modelling of sliding on boundaries of finite slope

yields much lower peak amplitude than suggested by the solution for infinitesimal boundary slope, and the peak is broadened and further reduced in height to order 10^{-2} by distributions of grain size and/or boundary viscosity (Lee and Morris, 2010; Lee et al., 2011). At much longer periods $T_o \sim \tau_d$, the regime of irrecoverable diffusionally accommodated grain-boundary sliding is expected within which it is predicted that $Q^{-1} \sim T_o$. For intermediate periods such that $\tau_e \ll T_o \ll \tau_d$, a regime of diffusionally-assisted grain-boundary sliding is predicted in which Q^{-1} varies mildly with period approximately as $T_o^{0.3}$. With increasing period within this regime, diffusion on progressively larger scales, ultimately approaching that of the grain size, erodes the grain-corner stress concentrations resulting from prior elastically accommodated sliding.

Experimental observations at high temperatures and relatively long periods reveal the generally weak monotonic variation of Q^{-1} with period, known as high-temperature background and broadly consistent with expectations for the diffusionally-assisted sliding regime. Under these circumstances, far from the elastic/anelastic threshold, the strain-energy dissipation and associated modulus dispersion may be adequately described as unique functions of a dimensionless period, that is the ratio of period to the Maxwell relaxation time i.e. $\tau_d = \eta\,(d,T)/G_U$. However, the growing body of experimental data at lower temperatures and correspondingly lower levels of dissipation $\sim 10^{-2}$, defy this simple parameterisation – suggesting that the characteristic timescale $\tau_e = \eta_{gb} d/G_U \delta$ for elastically accommodated sliding with its milder grain-size sensitivity must also be taken into account in an appropriate parameterisation of the viscoelastic behaviour. Experimental data for polycrystalline olivine tested in both steel and copper jackets at moderate temperatures provide so far circumstantial rather than definitive evidence for the existence of a broad dissipation peak or plateau and associated modest modulus dispersion tentatively attributed to elastically accommodated grain-boundary sliding. The results of complementary torsional microcreep tests show that for timescales of stress application comparable with seismic periods, much of the non-elastic strain is recoverable. This finding is consistent with significant roles for both elastically accommodated and diffusionally assisted grain-boundary sliding.

Resolution of these issues concerning extrapolation of data describing the viscoelastic behaviour of necessarily fine-grained laboratory materials to the much more coarse-grained rocks of the Earth's mantle is crucial for robust interpretation of seismological data. A comprehensive understanding of the role of grain-boundary sliding in the viscoelastic behaviour responsible for seismic wave dispersion and attenuation thus requires further experimental work. Particular targets should include forced-oscillation testing at the low levels of dissipation characteristic of low-moderate temperatures in fine-grained materials, including cleaner separation of the contributions of grain-boundary and intragranular (dislocation) relaxations. Complementary microcreep tests of longer duration, should be processed in parallel with forced-oscillation data for improved constraints on steady-state viscosities and the recoverability of non-elastic strain.

Acknowledgements

It is a real pleasure to dedicate this contribution to Professor Robert Liebermann – a mentor, colleague and friend of 40 year's standing! The experimental work described in this article was made possible by the contributions of Harri Kokkonen and Hayden Miller. The manuscript was substantially improved in response to thoughtful suggestions by Stephen Morris and two anonymous reviewers.

References

Anderson, O.L., Isaak, D.G., 1995. Elastic constants of mantle minerals at high temperature. In: Ahrens, T.J. (Ed.), Mineral Physics and Crystallography: A Handbook of Physical Constants. American Geophysical Union, pp. 64–97.

Ashby, M.F., 1972. Boundary defects and atomistic aspects of boundary sliding and diffusional creep. Surf. Sci. 31, 498–542.

Drury, M.R., Fitz Gerald, J.D., 1996. Grain-boundary melt films in an experimentally deformed olivine-orthopyroxene rock: implications for melt distribution in upper-mantle rocks. Geophys. Res. Lett. 73, 701–704.

Farla, R.J.M., Jackson, I., Fitz Gerald, J.D., Faul, U.H., Zimmerman, M.E., 2012. Dislocation damping and anisotropic seismic wave attenuation in Earth's upper mantle. Science 336, 332–335. http://dx.doi.org/10.1126/science.1218318.

Faul, U.H., Fitz Gerald, J.D., Jackson, I., 2004. Shear-wave attenuation and dispersion in melt-bearing olivine polycrystals II. Microstructural interpretation and seismological implications. J. Geophys. Res. 109, B06202. http://dx.doi.org/10.1029/2003JB002407.

Gribb, T.T., Cooper, R.F., 1998. Low-frequency shear attenuation in polycrystalline olivine: grain boundary diffusion and the physical significance of the Andrade model for viscoelastic rheology. J. Geophys. Res. 103 (B11), 27267–27279.

Hiraga, T., Anderson, I.M., Kohlstedt, D.L., 2003. Chemistry of grain boundaries in mantle rocks. Am. Mineral. 88, 1015–1019.

Jackson, I. 2000. Laboratory measurements of seismic wave dispersion and attenuation: recent progress, In: S. Karato et al. (Eds.), Earth's Deep Interior: Mineral Physics and Tomography from the Atomic to the Global Scale, AGU Geophys. Monogr. Ser. 117, 265–289.

Jackson, I., Faul, U.H., 2010. Grainsize-sensitive viscoelastic relaxation in olivine: towards a robust laboratory-based model for seismological application. Phys. Earth Planet. Inter. 183, 151–163. http://dx.doi.org/10.1016/j.pepi.2010.09.005.

Jackson, I., Fitz Gerald, J.D., Kokkonen, H., 2000. High-temperature viscoelastic relaxation in iron and its implications for the shear modulus and attenuation of the Earth's inner core. J. Geophys. Res. 105, 23605–23634.

Jackson, I., Faul, U.H., Fitz Gerald, J.D., Morris, S.J.S., 2006. Contrasting viscoelastic behaviour of melt-free and melt-bearing olivine: implications for the nature of grain-boundary sliding. Mat. Sci. Eng. A 442, 170–174.

Jackson, I., Barnhoorn, A., Aizawa, Y., Saint, C., 2009. Improved experimental procedures for the study of high-temperature viscoelastic relaxation. Phys. Earth Planet. Inter. 172, 104–115.

Kê, T., 1947. Experimental evidence of the viscous behaviour of grain boundaries in metals. Phys. Rev. 71 (8), 533–546.

Lakki, A., Schaller, R., Carry, C., 1998. High temperature anelastic and viscoplastic deformation of fine-grained MgO-doped Al_2O_3. Acta Mater. 46, 689–700.

Lee, L.C., Morris, S.J.S., 2010. Anelasticity and grain boundary sliding. Proc. R. Soc. A 2010 (466), 2651–2671. http://dx.doi.org/10.1098/rspa.2009.0624.

Lee, L.C., Morris, S.J.S., Wilkening, J., 2011. Stress concentrations, diffusionally accommodated grain boundary sliding and the viscoelasticity of polycrystals. Proc. R. Soc. A 467, 1624–1644. http://dx.doi.org/10.1098/rspa. 2010.0447.

Liebisch, T., 1891. Physikalische Krystallographie, viii, p. 614, 9 plates, Leipzig: Veit.

McCarthy, C., Takei, Y., Hiraga, T., 2011. Experimental study of attenuation and dispersion over a broad frequency range: 2. The universal scaling of polycrystalline materials. J. Geophys. Res. 116, B09207. http://dx.doi.org/10.1029/2011JB008384.

Morris, S.J.S., Jackson, I., 2009a. Diffusionally-assisted grain-boundary sliding and viscoelasticity of polycrystals. J. Mech. Phys. Solids 57, 744–761.

Morris, S.J.S., Jackson, I., 2009b. Implications of the similarity principle relating creep and attenuation in finely-grained solids. Mat. Sci. Eng. A. 521–522, 124–127.

Murase, T., McBirney, A.R., 1973. Properties of some common igneous rocks and their melts at high temperatures. Geol. Soc. Am. Bull. 84, 3563–3592.

Nowick, A.S., Berry, B.S., 1972. Anelastic Relaxation in Crystalline Solids. Academic Press, New York.

Pezzotti, G., 1999. Internal friction of polycrystalline ceramic oxides. Phys. Rev. B 60 (6), 4018–4029.

Raj, R., 1975. Transient behaviour of diffusion-induced creep and creep rupture. Metall. Trans. A 6A, 1499–1509.

Raj, R., Ashby, M.F., 1971. On grain boundary sliding and diffusional creep. Metall. Trans. 2, 1113–1127.

Sundberg, M., Cooper, R.F., 2010. A composite viscoelastic model for incorporating grain boundary sliding and transient diffusion creep; correlating creep and attenuation responses for materials with a fine grain size. Philos. Mag. 90 (20), 2817–2840.

Takei, Y., Karasawa, F., 2012. Experimental Study on Anelasticity of Polycrystalline Material for Seismological Application, Abstract T53D–07, Presented at 2012 Fall Meeting. AGU, San Francisco, California (3–7 Dec).

Voigt, W., 1883. Volumen- und winkeländerung krystallinischer körper all- oder einseitigem druck. Ann. Phys. 252, 416–427.